Knockdown of hsa_circ_0008922 inhibits the progression of glioma (#76739)

First submission

Guidance from your Editor

Please submit by **13 Oct 2022** for the benefit of the authors (and your token reward) .

Structure and Criteria
Please read the 'Structure and Criteria' page for general guidance.

Custom checks
Make sure you include the custom checks shown below, in your review.

Author notes
Have you read the author notes on the guidance page?

Raw data check
Review the raw data.

Image check
Check that figures and images have not been inappropriately manipulated.

Privacy reminder: If uploading an annotated PDF, remove identifiable information to remain anonymous.

Files

Download and review all files from the materials page.

9 Figure file(s)
6 Table file(s)
5 Raw data file(s)

! Custom checks

DNA data checks

- Have you checked the authors data deposition statement?
- Can you access the deposited data?
- Has the data been deposited correctly?
- Is the deposition information noted in the manuscript?

Human participant/human tissue checks

- Have you checked the authors ethical approval statement?
- Does the study meet our article requirements?
- Has identifiable info been removed from all files?
- Were the experiments necessary and ethical?

Cell line checks

Is the correct provenance of the cell line described?

For assistance email peer.review@peerj.com

Structure your review

The review form is divided into 5 sections. Please consider these when composing your review:

1. **BASIC REPORTING**
2. **EXPERIMENTAL DESIGN**
3. **VALIDITY OF THE FINDINGS**
4. General comments
5. Confidential notes to the editor

🗎 You can also annotate this PDF and upload it as part of your review

When ready [submit online](#).

Editorial Criteria

Use these criteria points to structure your review. The full detailed editorial criteria is on your [guidance page](#).

BASIC REPORTING

- Clear, unambiguous, professional English language used throughout.
- Intro & background to show context. Literature well referenced & relevant.
- Structure conforms to [PeerJ standards](#), discipline norm, or improved for clarity.
- Figures are relevant, high quality, well labelled & described.
- Raw data supplied (see [PeerJ policy](#)).

EXPERIMENTAL DESIGN

- Original primary research within [Scope of the journal](#).
- Research question well defined, relevant & meaningful. It is stated how the research fills an identified knowledge gap.
- Rigorous investigation performed to a high technical & ethical standard.
- Methods described with sufficient detail & information to replicate.

VALIDITY OF THE FINDINGS

- *i* Impact and novelty not assessed. *Meaningful* replication encouraged where rationale & benefit to literature is clearly stated.
- All underlying data have been provided; they are robust, statistically sound, & controlled.
- Conclusions are well stated, linked to original research question & limited to supporting results.

The best reviewers use these techniques

Tip	*Example*
Support criticisms with evidence from the text or from other sources	*Smith et al (J of Methodology, 2005, V3, pp 123) have shown that the analysis you use in Lines 241-250 is not the most appropriate for this situation. Please explain why you used this method.*
Give specific suggestions on how to improve the manuscript	*Your introduction needs more detail. I suggest that you improve the description at lines 57- 86 to provide more justification for your study (specifically, you should expand upon the knowledge gap being filled).*
Comment on language and grammar issues	*The English language should be improved to ensure that an international audience can clearly understand your text. Some examples where the language could be improved include lines 23, 77, 121, 128 – the current phrasing makes comprehension difficult. I suggest you have a colleague who is proficient in English and familiar with the subject matter review your manuscript, or contact a professional editing service.*
Organize by importance of the issues, and number your points	*1. Your most important issue* *2. The next most important item* *3. ...* *4. The least important points*
Please provide constructive criticism, and avoid personal opinions	*I thank you for providing the raw data, however your supplemental files need more descriptive metadata identifiers to be useful to future readers. Although your results are compelling, the data analysis should be improved in the following ways: AA, BB, CC*
Comment on strengths (as well as weaknesses) of the manuscript	*I commend the authors for their extensive data set, compiled over many years of detailed fieldwork. In addition, the manuscript is clearly written in professional, unambiguous language. If there is a weakness, it is in the statistical analysis (as I have noted above) which should be improved upon before Acceptance.*

Knockdown of hsa_circ_0008922 inhibits the progression of glioma

Chunhong Xue [Equal first author, 1], **Chang Liu** [Equal first author, 2, 3], **Xiang Yun** [4], **Xiaoqiong Zou** [1], **Xin Li** [1], **Ping Wang** [1], **Feng Li** [1], **Yingying Ge** [1, 5], **Qingmei Zhang** [1, 5], **Xiaoxun Xie** [1, 5, 6], **Xisheng Li** [Corresp., 7], **Bin Luo** [Corresp. 1, 5]

[1] Department of Histology and Embryology, School of Basic Medicine Science, Guangxi Medical University, Nanning, China

[2] Department of Neurosurgery, The first Affiliated Hospital of Guangxi Medical University, Nanning, China

[3] Postdoctoral Research Station, School of Basic Medicine Science, Guangxi Medical University, Nanning, China

[4] Department of International Cooperation and External Exchange, The first Affiliated Hospital of Guangxi Medical University, Nanning, China

[5] Key Laboratory of Preclinical Medicine (Guangxi Medical University), Education Department of Guangxi Zhuang Autonomous Region, Nanning, China

[6] Key Laboratory of Early Prevention and Treatment of Regional High Frequency Tumor (Guangxi Medical University), Ministry of Education, Nanning, China

[7] Department of Neurosurgery, The People's Hospital of Guangxi Zhuang Autonomous Region, Guangxi Academy of Medical Sciences, 6 Taoyuan Road, Nanning, China

Corresponding Authors: Xisheng Li, Bin Luo
Email address: lxssky@hotmail.com, glbinbin@sr.gxmu.edu.cn

Background: Glioma is a tumor originating from glial cells in the central nervous system. Although significant progress has been made in diagnosis and treatment, most high-grade glioma patients are prone to recurrence. Therefore, molecular targeted therapy may become a new direction for adjuvant therapy of glioma. In recent years, many studies have revealed that Circular RNA (circRNA) may play an important role in the occurrence and development of many tumors including glioams. Our previous study found that the expression of hsa_circ_0008922 was up-regulated in glioma tissues by RNA sequencing. However, the study of hsa_circ_0008922 in glioma has not yet been reported. Therefore, in this study, we preliminarily outline the expression of hsa_circ_0008922 in glioma and try to understand its biological functions. **Methods:** The expression of hsa_circ_0008922 in forty glioma tissues and four glioma cell lines (A172, U251, SF763 and U87) was detected by quantitative real-time polymerase chain reaction (qRT-PCR). The correlation between hsa_circ_0008922 expression and clinicopathological features of glioma patients was evaluated by Fisher's exact test. To understand the potential function of hsa_circ_0008922 in glioma, we constructed small interfering RNA (siRNA) of hsa_circ_0008922 to downregulate its expression in glioma cell lines A172 and U251. With these hsa_circ_0008922 downregulated cells, a series of assay was carried out as followed. Cell proliferation was detected by CCK8 assay, migration and invasion were determined by wound healing assay and transwell assay, respectively. And colony formation ability was evaluated by plate clonogenic assay. Moreover, flow cytometry combined with Western

Blot was performed to analyze apoptosis status and the expression of apoptotic related proteins (caspase 3 and caspase 9). Finally, the possible biological pathways and potential miRNA targets of hsa_circ_0008922 were predicted by bioinformatics. **Results:** We found that the expression of hsa_circ_0008922 in glioma tissues was higher than that in normal tissues. And the expression of hsa_circ_0008922 was related to the tumor grade of WHO classification, tumor size and Ki-67. After down-regulating the expression of hsa_circ_0008922, malignant biological behavior of glioma cells was inhibited, such as cell proliferation, colony formation, migration, and invasion. At the same time, it also induced apoptosis of glioma cells. Predicted analysis by bioinformatics demonstrated that hsa_circ_0008922 may be involved in tumor-related pathways by acting as a molecular sponge of multiple miRNAs (hsa-let-7e-5p, hsa-miR-506-5p, hsa-let-7b-5p, hsa-let-7c-5p and hsa-let-7a-5p). And we built a hsa_circ_0008922-miRNA-mRNA network.

1 **Manuscript Title**

2 **Knockdown of hsa_circ_0008922 inhibits the progression of glioma**

3 **Chun-Hong Xue[1, #], Chang Liu[2, 3#], Xiang Yun[4], Xiao-Qiong Zou[1], Xin Li[1], Ping Wang[1],**
4 **Feng Li[1], Ying-Ying Ge[1, 5], Qing-Mei Zhang[1, 5], Xiao-Xun Xie[1, 5, 6], Xi-Sheng Li[7, *], Bin Luo[1,**
5 **[5, *]**

6 [1]Department of Histology and Embryology, School of Basic Medicine Science, Guangxi Medical
7 University, Nanning, China.

8 [2]Department of Neurosurgery, The first Affiliated Hospital of Guangxi Medical University,
9 Nanning, China.

10 [3]Postdoctoral Research Station, School of Basic Medicine Science, Guangxi Medical University,
11 Nanning, China

12 [4]Department of International Cooperation and External Exchange, The first Affiliated Hospital of
13 Guangxi Medical University, Nanning, China.

14 [5]Key Laboratory of Preclinical Medicine (Guangxi Medical University), Education Department
15 of Guangxi Zhuang Autonomous Region, Nanning. China.

16 [6]Key Laboratory of Early Prevention and Treatment of Regional High Frequency Tumor
17 (Guangxi Medical University), Ministry of Education, Nanning China.

18 [7]Department of Neurosurgery, The People's Hospital of Guangxi Zhuang Autonomous Region,
19 Guangxi Academy of Medical Sciences, 6 Taoyuan Road, Nanning, China.

20 [#]These authors have contributed equally to this work.
21 https://orcid.org/0000-0002-4879-7923 (Chunhong Xue)
22
23 [*]Corresponding Author:
24 Xisheng Li
25 Department of Neurosurgery, The People's Hospital of Guangxi Zhuang Autonomous Region,
26 Guangxi Academy of Medical Sciences,6 Taoyuan Road, Nanning, China
27 E-mail: lxssky@hotmail.com
28 Bin Luo
29 Department of Histology and Embryology, School of Basic Medicine Science, Guangxi Medical
30 University,22 Shuangyong Road, Nanning, China
31 Email: glbinbin@sr.gxmu.edu.cn

Abstract

Background: Glioma is a tumor originating from glial cells in the central nervous system. Although significant progress has been made in diagnosis and treatment, most high-grade glioma patients are prone to recurrence. Therefore, molecular targeted therapy may become a new direction for adjuvant therapy of glioma. In recent years, many studies have revealed that Circular RNA (circRNA) may play an important role in the occurrence and development of many tumors including glioams. Our previous study found that the expression of hsa_circ_0008922 was up-regulated in glioma tissues by RNA sequencing. However, the study of hsa_circ_0008922 in glioma has not yet been reported. Therefore, in this study, we preliminarily outline the expression of hsa_circ_0008922 in glioma and try to understand its biological functions.

Methods: The expression of hsa_circ_0008922 in forty glioma tissues and four glioma cell lines (A172, U251, SF763 and U87) was detected by quantitative real-time polymerase chain reaction (qRT-PCR). The correlation between hsa_circ_0008922 expression and clinicopathological features of glioma patients was evaluated by Fisher's exact test. To understand the potential function of hsa_circ_0008922 in glioma, we constructed small interfering RNA (siRNA) of hsa_circ_0008922 to downregulate its expression in glioma cell lines A172 and U251. With these hsa_circ_0008922 downregulated cells, a series of assay was carried out as followed. Cell proliferation was detected by CCK8 assay, migration and invasion were determined by wound healing assay and transwell assay, respectively. And colony formation ability was evaluated by plate clonogenic assay. Moreover, flow cytometry combined with Western Blot was performed to analyze apoptosis status and the expression of apoptotic related proteins (caspase 3 and caspase 9). Finally, the possible biological pathways and potential miRNA targets of hsa_circ_0008922 were predicted by bioinformatics.

Results: We found that the expression of hsa_circ_0008922 in glioma tissues was higher than that in normal tissues. And the expression of hsa_circ_0008922 was related to the tumor grade of WHO classification, tumor size and Ki-67. After down-regulating the expression of hsa_circ_0008922, malignant biological behavior of glioma cells was inhibited, such as cell proliferation, colony formation, migration, and invasion. At the same time, it also induced apoptosis of glioma cells. Predicted analysis by bioinformatics demonstrated that hsa_circ_0008922 may be involved in tumor-related pathways by acting as a molecular sponge of multiple miRNAs (hsa-let-7e-5p, hsa-miR-506-5p, hsa-let-7b-5p, hsa-let-7c-5p and hsa-let-7a-5p). And we built a hsa_circ_0008922-miRNA-mRNA network.

Introduction

Glioma is one of the most common primary malignant tumors in the central nervous system. And glioblastoma multiforme (GBM) is the highest grade based on the WHO classification and has high invasiveness and lethality[1, 2]. Despite of improvements in current treatment modalities

72 (surgery, radiotherapy and chemotherapy)[3], the prognosis of GBM remains poor and the
73 recurrence rate still remain high after treatment[4, 5]. This poses a serious threat to the health of
74 patients and brings heavy economic burden to patients and their families. Therefore, it is critical
75 to identify potential molecules for adjuvant therapy option of glioma.
76
77 circRNA is a new class of non-coding RNAs with covalently closed-loop structures[6], which is
78 characterized by high stability and high conservation, and is mainly distributed in the cytoplasm.
79 In recent years, a variety of high-throughput sequencing confirmed that many circRNAs were
80 highly expressed in various tissues including tumors[7-9]. In addition, circRNA can also act as a
81 sponge for microRNAs (miRNA), endogenous competitive RNA to participate in many
82 pathophysiological processes[10]. Therefore, the expression profile and role of circRNA in
83 gliomas can not only provide a new treatment strategy, but also promote the development of
84 precision medicine in clinical diagnosis and treatment.
85
86 With RNA sequencing of a panel of glioma tissues and normal brain tissues we found
87 hsa_circ_0008922 was highly expression in glioma tissues compared with normal brain tissues.
88 As far as we know, there is only a report for hsa_circ_0008922 showing its abundant expression
89 in hypopharyngeal squamous cell carcinoma and correlation with worse outcome of patients[11].
90 So, we are very curious whether hsa_circ_0008922 has same feature in glioma. In this study, we
91 found that hsa_circ_0008922 expression was significantly associated with tumor grade, tumor
92 size and Ki-67. And the down-regulation of hsa_circ_0008922 expression in vitro can weaken
93 the malignant behavior of glioma cells, such as decreasing cell proliferation, migration, invasion
94 and inducing apoptosis. Additionally, bioinformatic analysis demonstrated that
95 hsa_circ_0008922 may exert a molecular sponge role for some miRNAs in glioma. Therefore,
96 these results provide a basis for further study of hsa_circ_0008922 in glioma in future.

Materials & Methods

Patients and samples

From May 2018 to November 2021, forty glioma specimens were collected in the Department of Neurosurgery, the First Affiliated Hospital of Guangxi Medical University and confirmed by the Department of pathology of same hospital. These patients did not receive radiotherapy or chemotherapy before surgery. And ten normal brain tissues were collected (Table 1). The above tissues were frozen in liquid nitrogen after in vitro. The specimen collection was examined and authorized by Medical Ethics Committee of Guangxi Medical University (2018087). We received written informed consent from participants of our study.

RNA Sequencing

All 10 human glioma tissues and 5 normal brain tissues were attained from patients who underwent surgery at The First Affiliated Hospital of Guangxi Medical University. To achieve five repeated samples at each group, a sample was taken from each of one patient to reduce the impact of individual differences. The 10 tissues were divided into two groups: NB (normal brain tissue, n = 5) and GBM (glioblastoma, n = 5). The total RNA from tissue of patients was extracted by the TRIzol reagent (Invitrogen, USA) and sequenced by Aksomics Biology Technology Co. Ltd (China). The RNA library was sequenced on the Illumina platform (Illumina, Santiago, CA, USA) and produced 150-bp pair-end reads. The NGS QC Toolkit (http:// www.nipgr.res.in/ngsqctoolkit.html) was used to process the raw data (the original reads) of FASTO format, and RPM (reads, mapped by splicing, per million) was taken as the expression of circRNA. Differential expression analysis was conducted using DESeq R package (Bioconductor.org). The circRNA with a P-value ≤ 0.05 and fold change $\geq$ or ≤ 1.5 was considered significantly differentially expressed. The statistical power of this experimental design, calculated in RNASeqPower using the web page at https://rodrigo-arcoverde.shinyapps.io/rnaseq_power_calc/ is 0.8083.

Cell culture and transfection

Human glioma cell lines (A172, U251, SF763 and U87) were purchased from the cell bank of the Chinese Academy of Sciences (Shanghai, China). Cells were cultured complete medium (10 % fetal bovine serum (Wisent, Canada); 1 % penicillin streptomycin (solarbio, Beijing); DMEM medium (Wisent, Canada)) and placed in 37 °C, 5 % CO_2 incubator.

Based on hsa_circ_0008922 sequence, two siRNAs (s1-hsa_circ_0008922 and s2-hsa_circ_0008922) and random siRNA (NC) fragments were ordered from Bioengineering Co., Ltd. (Shanghai, China). According to the instructions for siRNA usage, Lipofectamine 3000 (Invitrogen, CA, USA) was used to transfect siRNA into cells. The sequences of siRNA hsa_circ_0008922 as followed: s 1_hsa_circ_0008922：(sense) 5'-AAG AUA AGU AAC GAU GAC U-3', (antisense) 5'-AGU CAU CGU UAC UUA UCU U-3'; s2_hsa_circ_0008922：(sense) 5'-UAA CGA UGA CUU GAA AGU A-3', (antisense) 5'-UAC UUU CAA GUC AUC GUU A-3'.

137 ***qRT-PCR***
138 Total RNA was extracted by Vazyme Kit (RC101-01) (Vazyme, Nanjing, China). And RNA was
139 reverse transcribed into cDNA by HiScript III RT SuperMix 100 for qPCR (+gDNAwiper)
140 (Vazyme). ChamQSYBR qPCR Master Mix (Vazyme Q711-02) was used for polymerase chain
141 reaction in StepOne Real-time PCR System (Applied Biosystems, Foster City, CA, USA). The
142 relative level was calculated with $2^{-\Delta\Delta Ct}$.
143
144 ***RNase R exonuclease digestion experiment and electrophoresis***
145 According to the instructions of RNase R endonuclease digestion kit (Geneseed Biotech Co.,
146 Ltd., Guangzhou, China), the total RNA was divided into digestion group (RNase R treatment)
147 and control group, with 5 μg RNA (1 μg RNA required 8 U RNase R endonuclease digestion) in
148 each group. And the RNase R was not added in the control group. Above groups were incubated
149 at 37°C for 25 minutes Then 1 μg RNA was reversed and detected by qRT-PCR. The qRT-PCR
150 products amplified by the divergent primer were sent to Sangon Biotech (Shanghai) Co., Ltd. for
151 TA cloning sequencing to determine the full length of PCR products. The PCR products of
152 gDNA and cDNA were further detected by 1.3 % agarose gel electrophoresis. PCR products
153 were separated by 110 V electrophoresis for 35 min and detected by UV. GL DNA Marker 100
154 (AGbio, China) is used as a marker of DNA size. The sequences of primers are as followed:
155 hsa_circ_0008922 Divergent Primer: (sense) 5'-TCC ATC AGG ACC CCA GAT GTC-3',
156 (antisense) 5'-ACT GCA CAT GCA GAC TGT CAC-3'; hsa_circ_0008922 convergent Primer:
157 (sense) 5'-GGG CAT CCT TCA CCC ATC TG-3', (antisense) 5'-ATC TTG GTG TCA CAC
158 AGG GC-3'.
159
160 ***Wound Healing assay***
161 After transfection with siRNA of hsa_circ_0008922 for 48 hours, 100 μL of 2×10^4 cells were
162 seeded into the single hole of ibidi plug-in and cultured for 22 hours. After the cells were full of
163 ibidi plug-in, the plug-in was removed. Then DMEM complete medium was replaced with
164 appropriate low serum DMEM complete medium (2 % FBS). And photographs were taken at 0,
165 6, 12 hours and 0, 12, 24 hours, respectively.
166
167 ***CCK8 assay***
168 CCK8 detection kit (Vazyme A311-01) was used to detect the proliferation of glioma cells
169 treated with siRNA. 100 μL of 4×10^3 cells were inoculated in 96-well plates, 5 wells in each
170 group. 10 μL of CCK8 solution was added to each well and cells were incubated at 5 % CO_2 37
171 °C for 2 hours. The optical density (OD) values at 450 nm were measured at 0, 24, 48, 72 and 96
172 hours, respectively.
173
174
175 ***Transwell assay***
176 The migration and invasion ability of glioma cells were evaluated using transwell chamber

177 (Corning Incorporated, Corning, New York) with or without matrix glue (Absin). Forty-eight
178 hours after transfection, a 200μL cell suspension (2×10^4 cells) was inoculated in the upper
179 chamber of transwell chamber, and DMEM (500μL) containing 20 % FBS was added in the
180 lower chamber of transwell chamber. And they were incubated at 37 °C for 24 h. Then，4 %
181 methanol was applied to fix the cells for 30 min following by staining with 0.1 % Crystal Violet
182 Stain solution (Solarbio, Beijing, China) for 30 min. Staining cells were photographed by
183 inverted microscope (Olympus) and counted manually.
184
185 *Flow cytometry*
186 Apoptosis was detected by using FITC Annexin V apoptosis detection Kit (BD Biosciences
187 556547). After glioma cells were transfected, the cells were completely digested with EDTA-free
188 trypsin and washed twice with PBS buffered at 4 °C. The cells were dyed with 5 μL FITC
189 Annexin V and 5 μL propidium iodide (PI) for 15 min at room temperature in the dark and then
190 observed by flow cytometry (BD, USA). FlowjoV 1.8.1 (Becton, Dickinson& Company) was
191 used to analyze the results.
192
193 *Western Blot*
194 Western Blot was used to detect apoptosis-related proteins in glioma cells. After transfecting
195 siRNA into cells and culturing cells for 48 hours, the cells were harvested and lysed with
196 protease inhibitor and phosphatase inhibitor to extract proteins. Then, the protein was separated
197 by SDS-PAGE and transferred to PVDF membrane. 1: 1000 diluted primary antibodies (caspase
198 3, rabbit, #14220S; caspase 9, mouse, # 9508, Cell Signaling Technology and GAPDH, rabbit,
199 # ab181602 Abcam) were incubated overnight at 4 °C. After completing incubation of primary
200 antibodies, the secondary antibodies with 1: 5000 dilution were incubated at room temperature
201 (rabbit, # ab6721; mouse, # ab6728 Abcam).
202
203 *Plate cloning assay*
204 3×10^3 of siRNA treated cells were inoculated in the 6-well plates at 37 °C in 5 % CO_2 for 11
205 days. After culture, cells were fixed with 4 % formaldehyde for 30 min and stained with 0.1 %
206 Crystal Violet Stain solution for 12 min. And the photograph was recorded with a
207 stereomicroscope (Olympus).
208
209 *Bioinformatics analysis*
210 ENCORI (https://starbase.sysu.edu.cn/agoClipRNA.php?source=circRNA) was used to predict h
211 sa_circ_0008922 downstream miRNA. OECloud tools (https://cloud.oebiotech.cn/task/detail/arra
212 y_miranda_plot/?version=old) was used to predict binding fraction and free energy. miRDB (http:/
213 /mirdb.org/index.html), miRWalk (http://mirwalk.umm.uni-heidelberg.de/), Linkedomics (http://
214 linkedomics.org/login.php) were used to predict miRNA downstream mRNA, respectively. Cyto
215 scape was used to draw the interaction network of hsa_circ_0008922 with its downstream miRN
216 A, and the interaction network of miRNA with its downstream mRNA[12, 13]. GO (Gene Ontology)

217   and KEGG (Kyoto Encyclopedia of Genes and Genomes) enrichment analysis of miRNA downst
218   ream mRNA was performed on OECloud tools (https://cloud.oebiotech.cn/task/detail/enrichment
219   -oehw/?id=57).
220

221   ***Statistical analysis***
222   Data analysis was performed using Graphpad and SPSS 22.0 statistical analysis software.
223   Student's t-test was used for comparison between the experimental groups. Fisher's exact test
224   was used for categorical variables. Quantitative data were expressed as mean ± standard
225   deviation. $P < 0.05$ was considered statistically significant.

Results

Identifying hsa_circ_0008922 in glioma cell

In order to seek circRNA aberrantly expressed in glioma, we performed RNA sequence of glioma tissues. A total of 879 differentially expressed circRNAs (FDR<0.01, fold change>2 or <0.5) was gained, including 244 up-regulated and 655 down-regulated circRNAs. Here, we selected a novel circRNA, hsa_circ_0008922, from circRNA identified above due to that there was no report in glioma except only one study in hypopharyngeal squamous cell carcinoma[11]. As shown in Fig. 1A, hsa-circ-0008922 is produced from exon 3-4 of a human gene matrin 3 (MATR3, NM_199189) according to searching Circular RNA Interactome (https://circinteractome.nia.nih.gov/). The length of hsa_circ_0008922 spans from 92 bp to 252 bp on the sequence of MATR3.To evaluate the presence of hsa_circ_0008922 in glioma cells, firstly, RNase R was added to the total RNA extracted to remove the linear mRNA before cDNA synthesis based on the circRNA nature resistant to RNase R digestion. Then, we designed divergent primers for hsa_circ_0008922 and convergent primers for MATR3 mRNA. As shown in Fig. 1B, hsa_circ_0008922 can be amplified by divergent primers with cDNA as template, whereas there was no amplification detected at similar sizes using gDNA as template. Contrary, using convergent primers RT-PCR could amplify MATR3 mRNA in the sample without RNase R treatment, while it was failed to amplify MATR3 mRNA in the sample with RNase R treatment. Moreover, PCR products amplified by divergent primers were used for TA cloning and sequencing to confirm that hsa_circ_0008922 had the reverse splicing site (Fig. 1C). These results indicated that the divergent primers we designed can specifically amplify hsa_circ_0008922 and can used for detection of its expression.

Up-regulation of hsa_circ_0008922 in glioma tissues

Searching for five public databases of circRNA (ClRCpedia v2, http://yang-laboratory.com/circpedia/; circRNADb, http://reprod.njmu.edu.cn/cgi-bin/circrnadb/circRNADb.php; TSCD, http://gb.whu.edu.cn/TSCD/; MiOncoCirc, https://mioncocirc.github.io/; and circRNADisease, http://cgga.org.cn:9091/circRNADisease/), we cannot gain any information for the expression profile of hsa_circ_0008922 in glioma. Therefore, we tested our clinical samples as a primary study for hsa_circ_0008922 expression. As shown in Fig. 2A, the expression of hsa_circ_0008922 in glioma tissues (n=40) and normal tissues (n=10) was detected by qRT-PCR. We found that the relative expression of hsa_circ_0008922 was significantly higher in gliomas than in normal tissues (P=0.027). And it was found that in low-grade tumor and high-grade tumor the expression of hsa_circ_0008922 was significantly higher than normal tissues, respectively (Fig. 2B). Furthermore, we also detected the relative expression of hsa_circ_0008922 in different types of gliomas. We found that in astrocytoma and glioblastoma and oligodendroglioma the expression of hsa_circ_0008922 was higher than normal tissues, respectively (Fig. 2C).

263 *Correlation between hsa_circ_0008922 expression and clinicopathological parameters of*
264 *glioma patients*
265 As hsa_circ_0008922 was up-regulated in gliomas, we wonder whether it has some clinical
266 significance. Therefore, we further investigate the correlation between the expression of
267 hsa_circ_0008922 and clinical data such as age, gender, tumor size, WHO grade and GFAP
268 (glial fibrillary acidic protein). As shown in Table 2, the expression of hsa_circ_0008922 was
269 correlated with the WHO grade, tumor size and Ki-67 of patients. However, the expression of
270 hsa_circ_0008922 was not significantly correlated with other clinical parameters of patients.
271

272 *Screening highly efficient siRNA for hsa_circ_0008922*
273 Considering up-regulation of hsa_circ_0008922 correlating with some of clinicopathological
274 parameters of glioma patients, we further explore depletion of hsa_circ_0008922 to observe the
275 change of malignant behavior. We first detected the relative expression of hsa_circ_0008922 in a
276 panel of glioma cells (A172, U251, U87 and SF763 cells) by qRT-PCR. Fig. 3A shown all of
277 cells expressing hsa_circ_0008922 with different levels. A172 expressed the highest
278 hsa_circ_0008922, which was three times of SF763. Whereas U251 expressed the second higher
279 level of hsa_circ_000892 that was 1.6 times of SF763. As possessing high level of
280 hsa_circ_0008922 expression, A172 and U251 were selected for hsa_circ_0008922 depletion
281 cell models.
282

283 Subsequently, we determined the siRNA fragment and optimized its transfection time in vitro.
284 Transfecting cells with two siRNA fragments, s1-hsa_circ_0008922 and s2-hsa_circ_0008922,
285 respectively, it was found that s2-hsa_circ_0008922 had the best effect of -hsa_circ_0008922
286 down-regulation in the time point of forty-eight hours (Fig. 3B and C). Therefore, we chose s2-
287 hsa_circ_0008922 for hsa_circ_0008922 depletion experiments and set the forty-eight hours
288 after siRNA transfection to perform a series experiment for biological behavior in glioma cells.
289

290 *Inhibiting migration and invasion in glioma cells with down-regulated hsa_circ_0008922*
291 Because migration and invasion were closely related to the malignant degree of tumor, we used
292 wound healing assays to evaluate lateral migration of glioma cells. Through the analysis of time
293 series data and comparison between groups, it was found that the migration rate of s2-hsa_circ
294 _0008922 treatment group in A172 (Fig. 4A and C) and U251 (Fig. 4B and D) was lower than
295 that of the control. Further, the transwell assays of migration and invasion showed suppression of
296 longitudinal migration and invasion of A172 (Fig. 5A, B and C) and U251 (Fig. 5D, E and F)
297 following hsa-circ-0008922 silencing. In summary, the down-regulation of hsa_circ_0008922 in
298 glioma cells can significantly inhibit the migration and invasion ability of glioma cells.

299 *Influence of colony formation, proliferation, and apoptosis after hsa_circ_0008922 depletion*
300 *of glioma cells*
301 After down-regulating hsa_circ_0008922 in A172 and U251, the colony formation ability of
302 cells was detected by plate cloning. It was found that compared with the NC group, the number
303 of cell colonies in the s2-hsa_circ_0008922 group was significantly lower than that in the NC
304 group (Fig. 6A and B). CCK8 experiment was used to detect the proliferation of A172 and U251.
305 In this experiment, we detected cell viability at five time points (0 h, 24 h, 48 h, 72 h, 96 h). It
306 was found that the cell viability in the s2-hsa_circ_0008922 group in A172 (Fig. 6C) and U251
307 (Fig. 6D) was significantly different from that in the NC group. This result indicated that the
308 down-regulation of hsa_circ_0008922 in glioma cells can significantly inhibit the cell growth of
309 glioma cells.
310
311 Moreover, flow cytometry was used to study whether hsa_circ_0008922 affected the apoptosis
312 of glioma cells. We found that in A172 and U251, the apoptosis rate in the s2-hsa_circ_0008922
313 group was higher than that in the NC group, and there was significant indigenous difference
314 between the two groups ($p < 0.05$) (Fig. 7A and B and C). Furthermore, we also detected
315 apoptosis proteins caspase 3 and caspase 9. It was found that in A172 (Fig. 7D and E) and U251
316 (Fig. 7D and F) the expression of caspase 3 and caspase 9 in the s2-hsa_circ_0008922 group was
317 higher than those in the NC group, respectively. Taken together, hsa_circ_0008922 promoted the
318 proliferation of glioma cells by playing an anti-apoptotic role.
319
320 *Predicting hsa_circ_0008922-miRNA-mRNA networks with potential functions in glioma by*
321 *bioinformatics*
322 Generally, circRNA regulates gene transcription and expression by serving as a sponge of
323 miRNA. And circRNA-miRNA-mRNA regulatory axis has been widely accepted to illustrate the
324 biological functions of circRNA. To understand the potential function of hsa_circ_0008922 in
325 regulation of glioma related genes, we first analyzed miRNAs binding to hsa_circ_0008922 by
326 ENCORI, by which a total of 14 miRNAs (hsa-let-7e-5p, hsa-miR-506-5p, hsa-let-7b-5p, hsa-
327 let-7c-5p, hsa-let-7g-5p, hsa-mir-98-5p, hsa-let-7d-5p, hsa-let-7i-5p, hsa-miR-377-3p, hsa-mir-
328 605-3p, hsa-let-7a-5p, hsa-let-7f-5p, hsa-miR-4458 and hsa-miR-4500) were obtained (Fig. 8A).
329 Then, OECloud tools were used to predict the binding fraction and free energy of
330 hsa_circ_0008922 with its downstream miRNAs. The information of these miRNAs was
331 presented in table 3. The miRNAs (hsa-let-7e-5p, hsa-miR-506-5p, hsa-let-7b-5p, hsa-let-7c-5p
332 and hsa-let-7a-5p) with length greater than 22 bp, predicted score greater than 150 and predicted
333 free energy less than - 15 were selected for further bioinformatic analysis. With combined
334 analysis of three databases (miRDB, miRWalk and Linkedomics) we gained mRNAs that were
335 all related to glioma. As shown in Fig. 8B, 103 mRNAs interact with hsa-let-7a-5p, 123 mRNAs
336 interact with hsa-let-7b-5p, 99 mRNAs interact with hsa-let-7e-5p, 37 mRNAs interact with hsa-
337 let-7c-5p, and 5 mRNAs interact with hsa-miR-506-5p. Finally, an interactive network between
338 miRNA and mRNA was constructed (Fig. 8C).

339

340 Based on the ceRNA hypothesis, namely, mRNAs should be negatively correlated with targeted
341 miRNAs and positively correlated with circRNA. The top 30 of mRNAs fitting this criterion
342 were selected for further functional analysis. GO analysis showed that the functions of these
343 mRNAs were mainly related to multiple signaling pathways, such as mitotic sister chromatid
344 cohesion, stem cell population maintenance, negative regulation of intrinsic apoptotic signaling
345 pathway in response to DNA damage by p53 class mediator, negative regulation of cAMP-
346 mediated signaling, and regulation of transcription involved in G1/S transition of mitotic cell
347 cycle (Fig. 9A and Additional Table 1). And KEGG analysis indicated that these mRNAs were
348 involved in signaling pathways regulating pluripotency of stem cells, cell cycle, and microRNAs
349 in cancer and glioma (Fig. 9B and Additional Table 2).

350 **Discussion**

351 Glioma is a very common and aggressive intracranial tumor, which leads to brain dysfunction in
352 many patients and poses a serious threat to the health of patients. The World Health Organization
353 (WHO) divides glioma into four grades. Clinically, WHO I and WHO II grade gliomas were
354 defined as low grade glioma (LGG); whereas WHO III and WHO IV grade gliomas were
355 considered as high-grade glioma (HGG). And more than half of the gliomas in clinic are HGG
356 [14]. At present, the traditional treatment of glioma is the comprehensive treatment of surgery,
357 radiotherapy, and chemotherapy, but the prognosis is still poor, and the postoperative recurrence
358 rate is as high as 90%[4, 15, 16]. However, the pathogenesis and the progression of glioma still
359 remain unclear. Therefore, it is very important to understand the related molecules for their
360 expression features and their mechanisms in the occurrence and development of glioma.

361

362 With the development of high-throughput sequencing technology, it is found that about 50 % of
363 DNA in human genome can be transcribed into RNA, but the RNA with translational function
364 accounts for only 1.2 % of the transcribed RNA, and the RNA that cannot be translated into
365 protein is defined as non-coding RNA[17, 18]. Among them, a kind of non-coding RNA produced
366 by reverse splicing of precursor mRNA (pre-mRNA) is called circRNA[19]. In early studies,
367 circRNA was considered as "noise" and had no biological function. However, in recent years, it
368 was found that circRNAs mostly distributed in the brain and had significant biological functions,
369 especially in cancer[20-22]. In 2019, Xia et al. showed that AKT3-174aa encoded by circ-AKT3
370 could inhibit the carcinogenicity of glioma mother cells[23]. In 2020, Peng et al. reported that
371 circ-MAPK4 was up-regulated in glioma, but its expression in high-grade glioma was
372 significantly higher than that in low-grade glioma[24]. At the same time, Chen et al. found that the
373 expression level of hsa_circ_0074026 was significantly increased in the parent cell samples and
374 cells of glioma, and was correlated with clinical parameters such as tumor size, WHO grade and
375 overall survival[25]. All of these reports imply circRNA has potential for diagnostic and
376 therapeutic application in gliomas. However, there are still less information about a circRNA in
377 glioma.

378

379   Through RNA sequencing, we found that hsa_circ_0008922 highly expressed in glioma tissues.
380   hsa_circ_0008922 is derived from exon 3 and exon 4 of Matrin3 (MATR3). MATR3 is a host
381   gene of hsa_circ_0008922 and it is derived from human chromosome 5 and highly expresses in
382   the brain[26]. MATR3 participates in many cellular processes, including binding and stabilizing
383   mRNA, regulating mRNA nuclear output, chromatin remodeling, RNA processing, transcription,
384   translation, and apoptosis[11, 27]. In addition, MATR3 has been widely studied in amyotrophic
385   lateral sclerosis[28-30]. However, the research progressed on circRNA from MATR3 in glioma
386   remains unreported. In this study, we first verified that the expression of hsa_circ_0008922 in
387   glioma tissues was higher than that in normal tissues. Statistical analysis showed that the
388   expression of hsa_circ_0008922 was significantly correlated with WHO grade, indicating that
389   hsa_circ_0008922 could be a significant role in the progression of malignant glioma. And the
390   expression of hsa_circ_0008922 was significantly correlated with tumor size and Ki-67, which
391   indicated that hsa_circ_0008922 could have a significant function in proliferation of glioma cells.
392   Down-regulation of hsa_circ_0008922 expression in glioma cell lines A172 and U251 can
393   significantly inhibit the proliferation, migration, and invasion of the two cells, indicating that
394   hsa_circ_0008922 may become a new molecule for molecular targeted therapy.
395

396   Previous studies have shown that circRNA is often used as a miRNA sponge to regulate the
397   expression of miRNA in various cancers, forming a circRNA-miRNA-mRNA network to
398   regulate the expression of downstream target genes and affect the development of cancer[31, 32].
399   For example, hsa_circ_0003222 promoted stem cell differentiation and progression of non-small
400   cell lung cancer through miR-527[33]. Therefore, in this study, we predicted miRNAs regulated
401   by hsa_circ_0008922 through bioinformatics analysis, and selected 5 miRNAs for bioinformatics
402   prediction based on predicted binding fraction and free energy. Previous studies have shown that
403   hsa-let-7b-5p, hsa-let-7e-5p and hsa-let-7c-5p were all tumor suppressors. In 2019, Xi et al.
404   found that hsa-let-7b-5p could inhibit the migration, invasion, and cell cycle of glioma cells[34].
405   Another study found that hsa-let-7e-5p as a tumor suppressor could inhibit the progression of
406   head and neck squamous cell carcinoma by targeting CCR7 expression[35]. A study reported by
407   Fu et al in 2017 demonstrated that hsa-let-7c-5p may act as a tumor suppressor of breast cancer
408   by negatively regulating ERCC6, providing a new strategy for breast cancer treatment[36]. Thus，
409   the interaction between the hsa_circ_0008922 and these three members of the hsa-let-7 miRNA
410   family may broaden our view for their functions in glioma.
411

412   It was interested that a gene called DNA polymerase lambda (POLL) may be regulated by above
413   mentioned three miRNAs (hsa-let-7b-5p, hsa-let-7e-5p and hsa-let-7c-5p), simultaneously, and
414   its expression may be negatively correlated with the expression of these three miRNAs. Now,
415   there is a report that POLL is differentially expressed in IDH (lactate dehydrogenase) mutant and
416   wild type carriers, relating to the survival rate of patients with LGG[37]. In future, a series of
417   experiments such as RIP (RNA Binding Protein Immunoprecipitation Assay), RNA pull-down
418   assay and luciferase reporter gene assay have to be performed to illustrate the complicate

419   function of hsa_circ_0008922 in this circRNA-miRNA-mRNA network.

420

421   We performed GO analysis and KEGG analysis on the target genes negatively correlated with 5
422   miRNAs, and the results showed that hsa_circ_0008922 regulates cancer-related functions and
423   signaling pathways by regulating several miRNAs to play a carcinogenic role. GO analysis
424   showed that the enriched functions of mRNA negatively correlated with miRNAs were mainly
425   related to cell cycle, including regulation of transcription involved in G1/S transition of mitotic
426   cell cycle and mitotic sister chromatid cohesion. Enriched functions were also demonstrated in
427   relating to apoptosis, including negative regulation of intrinsic apoptotic signaling pathway in
428   response to DNA damage by p53 class mediator[38, 39], negative regulation of cAMP-mediated
429   signaling[40]. In the result of KEGG analysis, enriched pathways of mRNA negatively correlated
430   with miRNAs were mainly related to tumor, e. g. microRNAs in cancer signaling pathway,
431   glioma signaling pathway. It was also included in cell cycle signaling pathway, Ras signaling
432   pathway[41], AMPK signaling pathway[42], and mTOR signaling pathway[43]. However, it needs to
433   further confirmation.

434

435   In summary, this is first time to report the up-regulated hsa_circ_0008922 in glioma and use
436   bioinformatics to analyze the possible biological processes and signaling pathways regulated by
437   hsa_circ_0008922. This study may provide a future direction for further studying
438   hsa_circ_0008922 in the auxiliary diagnosis and treatment of glioma.

439

Conclusions

441   Glioma highly expressed hsa_circ_0008922, which could affect the proliferation, migration, and
442   apoptosis of glioma cells. And hsa_circ_0008922 may server as a sponge for multiple miRNAs.

443

Acknowledgements

451

References

453   [1]   Ng S, Zouaoui S, Bessaoud F, et al. An Epidemiology Report for Primary Central Nervous System Tumors
454   in Adolescents and Young Adults: A Nationwide Population-Based Study in France, 2008-2013 [J]. Neuro-oncology,
455   2020, 22(6): 851-863.
456   [2]   Sminia P, Van Den Berg J, Van Kootwijk A, et al. Experimental and Clinical Studies on Radiation and
457   Curcumin in Human Glioma [J]. Journal of cancer research and clinical oncology, 2021, 147(2): 403-409.
458   [3]   Nabors L B, Portnow J, Ahluwalia M, et al. Central Nervous System Cancers, Version 3.2020, Nccn
459   Clinical Practice Guidelines in Oncology [J]. Journal of the National Comprehensive Cancer Network : JNCCN,
460   2020, 18(11): 1537-1570.

461 [4]   Deangelis L M. Brain Tumors [J]. The New England journal of medicine, 2001, 344(2): 114-123.

462 [5]   Francis S S, Ostrom Q T, Cote D J, et al. The Epidemiology of Central Nervous System Tumors [J].
463 Hematology/oncology clinics of North America, 2022, 36(1): 23-42.

464 [6]   Cocquerelle C, Mascrez B, Hétuin D, et al. Mis-Splicing Yields Circular Rna Molecules [J]. FASEB
465 journal : official publication of the Federation of American Societies for Experimental Biology, 1993, 7(1): 155-160.

466 [7]   Xu Y, Yao Y, Liu Y, et al. Elevation of Circular Rna Circ_0005230 Facilitates Cell Growth and Metastasis
467 Via Sponging Mir-1238 and Mir-1299 in Cholangiocarcinoma [J]. Aging, 2019, 11(7): 1907-1917.

468 [8]   Xu Y, Yao Y, Zhong X, et al. Downregulated Circular Rna Hsa_Circ_0001649 Regulates Proliferation,
469 Migration and Invasion in Cholangiocarcinoma Cells [J]. Biochemical and biophysical research communications,
470 2018, 496(2): 455-461.

471 [9]   Starke S, Jost I, Rossbach O, et al. Exon Circularization Requires Canonical Splice Signals [J]. Cell reports,
472 2015, 10(1): 103-111.

473 [10]   Sun J, Li B, Shu C, et al. Functions and Clinical Significance of Circular Rnas in Glioma [J]. Molecular
474 cancer, 2020, 19(1): 34.

475 [11]   Wang Z, Wei P, Wei D, et al. Effect of up-Regulation of Circmatr3 on the Proliferation, Metastasis,
476 Progression and Survival of Hypopharyngeal Carcinoma [J]. Journal of cellular and molecular medicine, 2020, 24(8):
477 4687-4697.

478 [12]   Shannon P, Markiel A, Ozier O, et al. Cytoscape: A Software Environment for Integrated Models of
479 Biomolecular Interaction Networks [J]. Genome research, 2003, 13(11): 2498-2504.

480 [13]   Assenov Y, Ramírez F, Schelhorn S E, et al. Computing Topological Parameters of Biological Networks
481 [J]. Bioinformatics (Oxford, England), 2008, 24(2): 282-284.

482 [14]   Ostrom Q T, Cioffi G, Gittleman H, et al. Cbtrus Statistical Report: Primary Brain and Other Central
483 Nervous System Tumors Diagnosed in the United States in 2012-2016 [J]. Neuro-oncology, 2019, 21(Suppl 5): v1-
484 v100.

485 [15]   Ostrom Q T, Bauchet L, Davis F G, et al. The Epidemiology of Glioma in Adults: A "State of the Science"
486 Review [J]. Neuro-oncology, 2014, 16(7): 896-913.

487 [16]   Van Meir E G, Hadjipanayis C G, Norden A D, et al. Exciting New Advances in Neuro-Oncology: The
488 Avenue to a Cure for Malignant Glioma [J]. CA: a cancer journal for clinicians, 2010, 60(3): 166-193.

489 [17]   Liu W, Tao J C, Zhu S Z, et al. Expression and Regulatory Network of Long Noncoding Rna in Rats after
490 Spinal Cord Hemisection Injury [J]. Neural regeneration research, 2022, 17(10): 2300-2304.

491 [18]   Jarroux J, Morillon A, Pinskaya M. History, Discovery, and Classification of Lncrnas [J]. Advances in
492 experimental medicine and biology, 2017, 1008(1-46.

493 [19]   Liang Q, Li X, Guan G, et al. Long Non-Coding Rna, Hotairm1, Promotes Glioma Malignancy by Forming
494 a Cerna Network [J]. Aging, 2019, 11(17): 6805-6838.

495 [20]   Shahzad U, Krumholtz S, Rutka J T, et al. Noncoding Rnas in Glioblastoma: Emerging Biological
496 Concepts and Potential Therapeutic Implications [J]. Cancers, 2021, 13(7):

497 [21]   Yang Y, Gao X, Zhang M, et al. Novel Role of Fbxw7 Circular Rna in Repressing Glioma Tumorigenesis
498 [J]. Journal of the National Cancer Institute, 2018, 110(3): 304-315.

499 [22]   Rybak-Wolf A, Stottmeister C, Glažar P, et al. Circular Rnas in the Mammalian Brain Are Highly
500 Abundant, Conserved, and Dynamically Expressed [J]. Molecular cell, 2015, 58(5): 870-885.

501 [23]   Xia X, Li X, Li F, et al. A Novel Tumor Suppressor Protein Encoded by Circular Akt3 Rna Inhibits
502 Glioblastoma Tumorigenicity by Competing with Active Phosphoinositide-Dependent Kinase-1 [J]. Molecular
503 cancer, 2019, 18(1): 131.

504 [24]   He J, Huang Z, He M, et al. Circular Rna Mapk4 (Circ-Mapk4) Inhibits Cell Apoptosis Via Mapk
505 Signaling Pathway by Sponging Mir-125a-3p in Gliomas [J]. Molecular cancer, 2020, 19(1): 17.

506 [25]   Chen M, Liu X, Xie P, et al. Circular Rna Circ_0074026 Indicates Unfavorable Prognosis for Patients with
507 Glioma and Facilitates Oncogenesis of Tumor Cells by Targeting Mir-1304 to Modulate Erbb4 Expression [J].
508 Journal of cellular physiology, 2020, 235(5): 4688-4697.

509 [26]   Coelho M B, Attig J, Ule J, et al. Matrin3: Connecting Gene Expression with the Nuclear Matrix [J]. Wiley
510 interdisciplinary reviews RNA, 2016, 7(3): 303-315.

511 [27]   Salem A, Wilson C J, Rutledge B S, et al. Matrin3: Disorder and Als Pathogenesis [J]. Frontiers in
512 molecular biosciences, 2021, 8(794646.

513 [28]   You J, Maksimovic K, Lee J, et al. Selective Loss of Matr3 in Spinal Interneurons, Upper Motor Neurons
514 and Hippocampal Ca1 Neurons in a Matr3 S85c Knock-in Mouse Model of Amyotrophic Lateral Sclerosis [J].
515 Biology, 2022, 11(2):

516 [29]   Cavalli M, Cardani R, Renna L V, et al. First Family of Matr3-Related Distal Myopathy from Italy: The

517 Role of Muscle Biopsy in the Diagnosis and Characterization of a Still Poorly Understood Disease [J]. Frontiers in
518 neurology, 2021, 12(715386.
519 [30]   Van Bruggen R, Maksimovic K, You J, et al. Matr3 F115c Knock-in Mice Do Not Exhibit Motor Defects
520 or Neuropathological Features of Als [J]. Biochemical and biophysical research communications, 2021, 568(48-54.
521 [31]   Hansen T B, Jensen T I, Clausen B H, et al. Natural Rna Circles Function as Efficient Microrna Sponges [J].
522 Nature, 2013, 495(7441): 384-388.
523 [32]   Kristensen L S, Hansen T B, Venø M T, et al. Circular Rnas in Cancer: Opportunities and Challenges in the
524 Field [J]. Oncogene, 2018, 37(5): 555-565.
525 [33]   Li C, Zhang J, Yang X, et al. Hsa_Circ_0003222 Accelerates Stemness and Progression of Non-Small Cell
526 Lung Cancer by Sponging Mir-527 [J]. Cell death & disease, 2021, 12(9): 807.
527 [34]   Xi X, Chu Y, Liu N, et al. Joint Bioinformatics Analysis of Underlying Potential Functions of Hsa-Let-7b-
528 5p and Core Genes in Human Glioma [J]. Journal of translational medicine, 2019, 17(1): 129.
529 [35]   Wang S, Jin S, Liu M D, et al. Hsa-Let-7e-5p Inhibits the Proliferation and Metastasis of Head and Neck
530 Squamous Cell Carcinoma Cells by Targeting Chemokine Receptor 7 [J]. Journal of Cancer, 2019, 10(8): 1941-
531 1948.
532 [36]   Fu X, Mao X, Wang Y, et al. Let-7c-5p Inhibits Cell Proliferation and Induces Cell Apoptosis by Targeting
533 Ercc6 in Breast Cancer [J]. Oncology reports, 2017, 38(3): 1851-1856.
534 [37]   Pang F M, Yan H, Mo J L, et al. Integrative Analyses Identify a DNA Damage Repair Gene Signature for
535 Prognosis Prediction in Lower Grade Gliomas [J]. Future oncology (London, England), 2020, 16(8): 367-382.
536 [38]   Khan M R, Bukhari I, Khan R, et al. Tp53lnc-Db, the Database of Lncrnas in the P53 Signalling Network
537 [J]. Database : the journal of biological databases and curation, 2019, 2019(
538 [39]   Riley T, Sontag E, Chen P, et al. Transcriptional Control of Human P53-Regulated Genes [J]. Nature
539 reviews Molecular cell biology, 2008, 9(5): 402-412.
540 [40]   Jiang K, Yao G, Hu L, et al. Mob2 Suppresses Gbm Cell Migration and Invasion Via Regulation of
541 Fak/Akt and Camp/Pka Signaling [J]. Cell death & disease, 2020, 11(4): 230.
542 [41]   Downward J. Ras Signalling and Apoptosis [J]. Current opinion in genetics & development, 1998, 8(1): 49-
543 54.
544 [42]   Mihaylova M M, Shaw R J. The Ampk Signalling Pathway Coordinates Cell Growth, Autophagy and
545 Metabolism [J]. Nature cell biology, 2011, 13(9): 1016-1023.
546 [43]   Yu J S, Cui W. Proliferation, Survival and Metabolism: The Role of Pi3k/Akt/Mtor Signalling in
547 Pluripotency and Cell Fate Determination [J]. Development (Cambridge, England), 2016, 143(17): 3050-3060.
548

Figure legends

550 **Figure 1 Identify hsa_circ_0008922.** (A) Schematic diagram of the ring formation mechanism

551 of hsa_circ_0008922. (B) Agarose gel electrophoresis was used to detect the stability of

552 hsa_circ_0008922. M is DNA marker. RNase R$^+$ represents RNA treated with RNase.R. RNase

553 R$^-$ represents RNA treated without RNase.R. "◄►" represents divergent primers. "►◄" represents

554 convergent primers. (C) NCBI Blast was used to compare the consistency of PCR product

555 sequencing results with the target sequence. Arrows and red line segments indicate

556 circularization sites.

557

558 **Figure 2 hsa_circ_0008922 expression in glioma tissues by qRT-PCR** (A) The expression of

559 hsa_circ_0008922 in glioma tissues (n=40) were compared as normal brain tissues (n=10). (B)

560 The expression of hsa_circ_0008922 was investigated between the groups of normal brain

561 tissues (n=10), low-grade tumor (n=20) and high-grade tumor (n=20). (C) The expression of

562 hsa_circ_0008922 was analyzed in different pathological types of glioma (normal brain tissues

563 n=10, astrocytoma n=23, glioblastoma n=15, oligodendroglioma n=2). Data is expressed as mean

564 ± SEM. P < 0.05.

565

566 **Figure 3 Identify hsa_circ_0008922 expression in glioma cell lines and select siRNA**

567   **fragments.** (A) The relative expression of hsa_circ_0008922 in common glioma cell lines
568   (SF763, U87, U251, A172) was detected. (B and C) The hsa_circ_0008922 was down-regulated
569   in A172 and U251 cells, and the knock-down efficiency of the two siRNA fragments was
570   detected at 48 h and 72 h. s1-hsa_circ_0008922 and s2-hsa_circ_0008922 represent two siRNA
571   fragments. Data is expressed as mean ± SEM. **$P < 0.01$, ***$P < 0.001$, ns indicates no
572   statistically significant difference.
573
574   **Figure 4 hsa_circ_0008922 regulates wound healing of A172 and U251 cells.** (A and B) After
575   down-regulation of hsa_circ_0008922 in A172, the scratch images at different time points were
576   taken. (C and D) The quantitative results of scratch experiments in the NC group and the s2-
577   has_circ_0008922 group in the A172 and U251 were counted. The ordinate is healing rate. The
578   abscissa is the detection time point. s2-has_circ_0008922 represents the second siRNA
579   fragments. Data is expressed as mean ± SEM. **$P < 0.01$, ***$P < 0.001$.
580
581   **Figure 5 hsa_circ_0008922 attenuated migration and invasion of A172 and U251 cells.** (A a
582   nd D) After down-regulation of hsa_circ_0008922 in A172 and U251, the graphs of migration an
583   d invasion were taken. (B, C, D and F) After down-regulating hsa_circ_0008922 in A172 and U2
584   51, the quantitative results of migration and invasion experiments in NC group and s2-hsa_circ_0
585   008922 group were counted. The vertical axis is the number of cells. s2-has_circ_0008922 repres
586   ents the second siRNA fragments. Data is expressed as mean ± SEM. *$P < 0.05$, **$P < 0.01$.
587
588   **Figure 6 Down-regulation of hsa_circ_0008922 inhibited the colony formation and cell**
589   **viability of A172 and U251 cells.** (A and B) Cell colony formation was detected by plate
590   cloning after has_circ_0008922 was down-regulated in A172 and U251. (C and D) After down-
591   regulating has_circ_0008922 in A172 and U251, cell viability was detected by CCK8. The
592   ordinate is OD value. The abscissa is the detection time point (0 h, 24 h, 48 h, 72 h, 96 h). s2-
593   has_circ_0008922 represents the second siRNA fragments. Data is expressed as mean ± SEM.
594   *$P < 0.05$, **$P < 0.01$.
595
596   **Figure 7 Down-regulation of hsa_circ_0008922 inhibited apoptosis of A172 and U251**
597   **cells.**(A) Cell apoptosis was detected by flow cytometry after down-regulation of
598   has_circ_0008922 in A172 and U251. (B and C) The apoptosis results of A172 and U251 were
599   calculated. The ordinate is the apoptosis rate. (D) After down-regulating has_circ_0008922 in
600   A172 and U251, WB was used to detect apoptosis-related protein expression. (E and F) The
601   quantification results of A172 and U251 apoptosis protein were analyzed. The ordinate is the
602   relative protein expression. The abscissa is the detected protein. s2-has_circ_0008922 represents
603   the second siRNA fragments. Data is expressed as mean ± SEM. **$P < 0.01$, ***$P < 0.001$.
604
605   **Figure 8 Prediction of the networks of circRNA-miRNA-mRNA.** (A) The interaction network
606   between hsa_circ_0008922 and its downstream miRNAs was constructed. The blue square
607   represents hsa_circ_0008922. Red circles indicate miRNAs. The line segment between the blue
608   square and the red circle indicates a targeting relationship. The darker the line segment, the lower
609   the predicted free energy, and the wider the line segment, the higher the predicted binding score.
610   (B) Veen plots of mRNAs interacting with miRNAs downstream of hsa_circ_0008922 were
611   drawn. Numbers in red circles indicate the number of mRNAs interacting with miRNAs in
612   Linkedomics. Numbers in blue circles indicate the number of mRNAs interacting with miRNAs

613   in miRDB. Numbers in green circles indicate the number of mRNAs interacting with miRNAs in
614   miRWalk. (C) The interaction network between miRNA and its interacting mRNA was
615   constructed. Red represents miRNA. white and blue represent mRNA; The larger the red circle,
616   the higher the number of mRNAs interacting with the miRNA. The darker the circle, the higher
617   the number of miRNAs interacting with the mRNA. The red line segment represents a positive
618   correlation, and the wider the line segment, the stronger the positive correlation. The blue line
619   segment represents a negative correlation, and the wider the line segment, the stronger the
620   negative correlation.
621
622   **Figure 9 Analysis of the function of mRNAs negatively correlated with miRNAs.** (A) A
623   bubble plot of the top 30 enriched GO terms in mRNAs negatively correlated with miRNAs
624   downstream of hsa_circ_0008922 was drawn. The y-axis represents the enrichment of the top 30
625   items, and the x-axis represents the enrichment score. The size of the bubbles indicates the
626   number of mRNAs in the GO term. Bubble colors represent p-values. (B) A bubble plot of the
627   top 30 enriched pathways in mRNAs negatively correlated with miRNAs downstream of
628   hsa_circ_0008922 was drawn. The y-axis represents the enrichment of the top 30 items, and the
629   x-axis represents the enrichment score. The size of the bubbles indicates the number of mRNAs
630   in the pathway. Bubble colors represent p-values.

Figure 1

Identify hsa_circ_0008922

(A) Schematic diagram of the ring formation mechanism of hsa_circ_0008922. (B) Agarose gel electrophoresis was used to detect the stability of hsa_circ_0008922. M is DNA marker.

RNase R$^+$ represents RNA treated with RNase.R. RNase R$^-$ represents RNA treated without RNase.R. "◀▶" represents divergent primers. "▶◀" represents convergent primers. (C) NCBI Blast was used to compare the consistency of PCR product sequencing results with the target sequence. Arrows and red line segments indicate circularization sites.
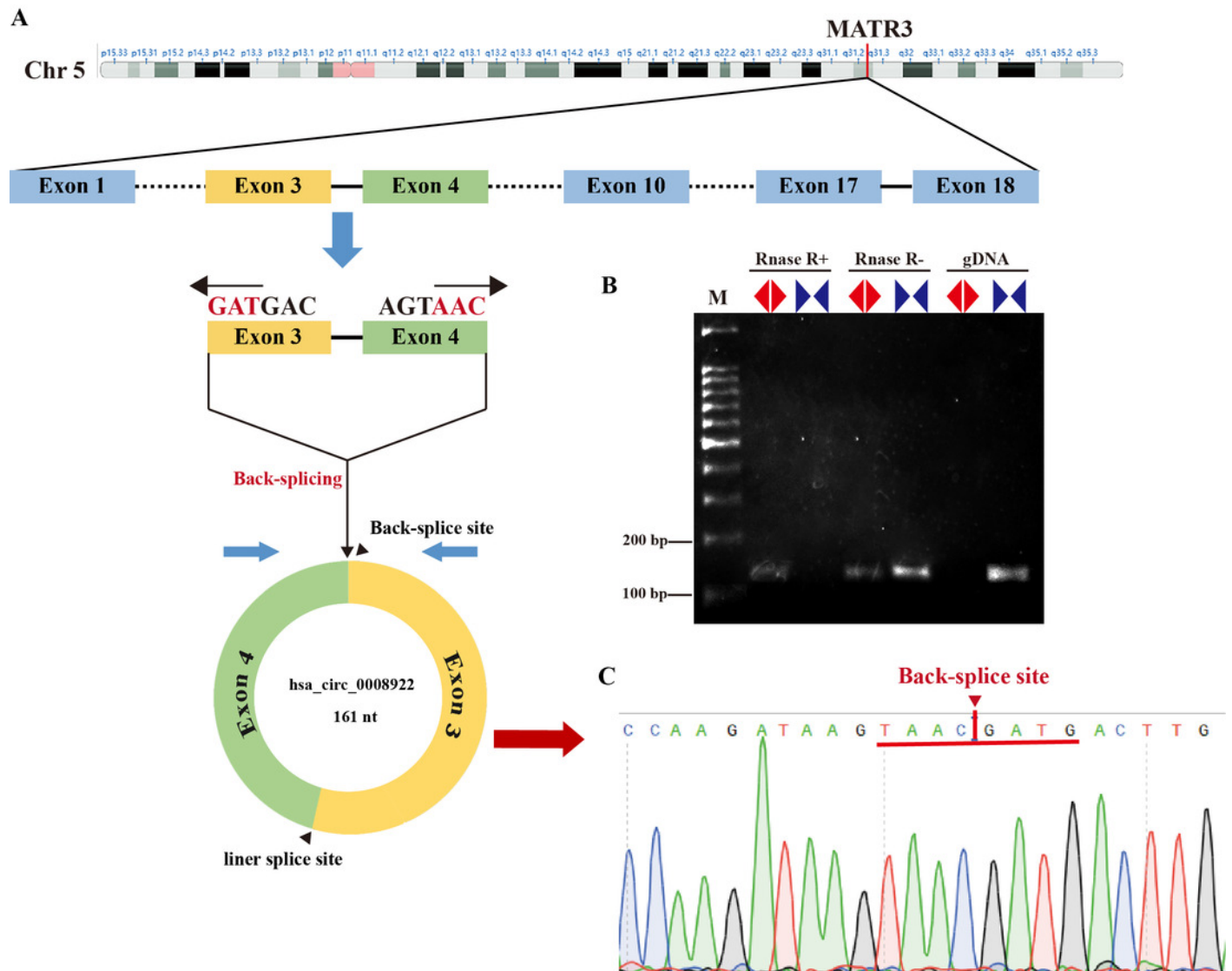
Figure 2

hsa_circ_0008922 expression in glioma tissues by qRT-PCR

(A) The expression of hsa_circ_0008922 in glioma tissues (n=40) were compared as normal brain tissues (n=10). (B) The expression of hsa_circ_0008922 was investigated between the groups of normal brain tissues (n=10), low-grade tumor (n=20) and high-grade tumor (n=20). (C) The expression of hsa_circ_0008922 was analyzed in different pathological types of glioma (normal brain tissues n=10, astrocytoma n=23, glioblastoma n=15, oligodendroglioma n=2). Data is expressed as mean ± SEM. $P < 0.05$.
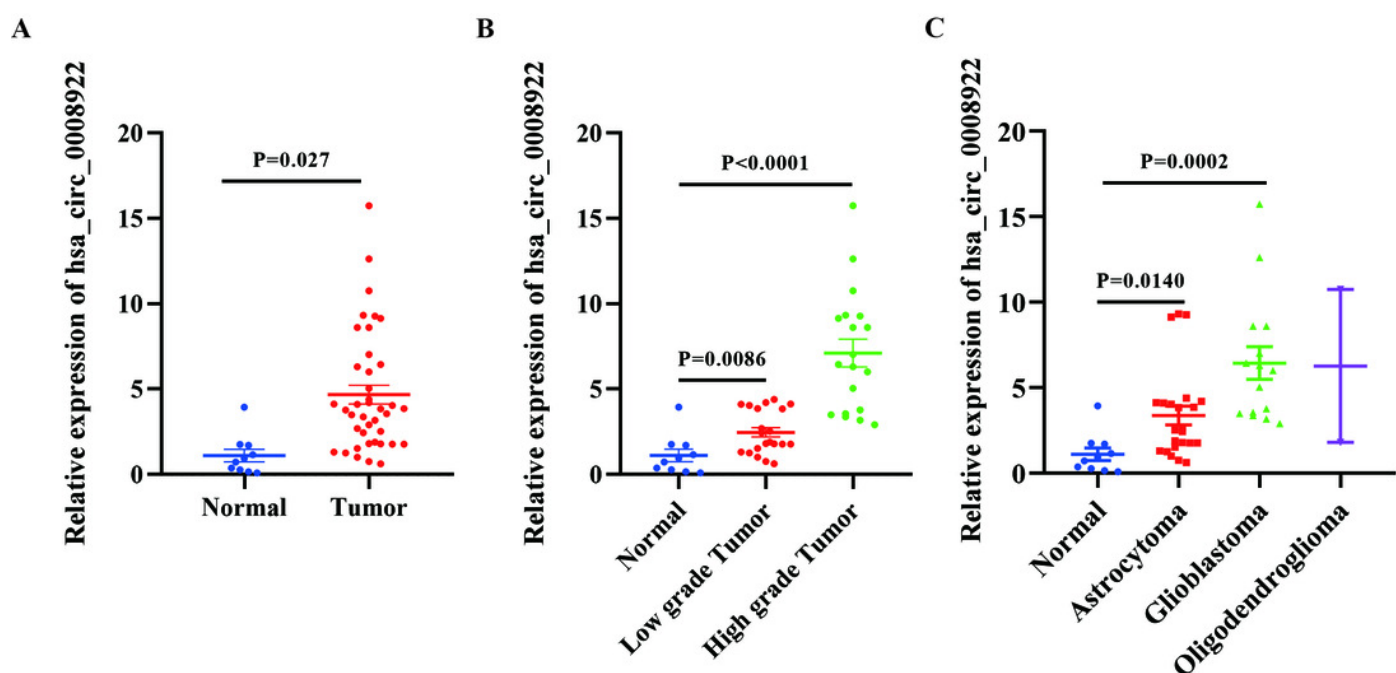
Figure 3

Identify hsa_circ_0008922 expression in glioma cell lines and select siRNA fragments.

(A) The relative expression of hsa_circ_0008922 in common glioma cell lines (SF763 , U87, U251, A172) was detected. (B and C) The hsa_circ_0008922 was down-regulated in A172 and U251 cells, and the knock-down efficiency of the two siRNA fragments was detected at 48 h and 72 h. s1-hsa_circ_0008922 and s2-hsa_circ_0008922 represent two siRNA fragments. Data is expressed as mean ± SEM. **$P < 0.01$, ***$P < 0.001$, ns indicates no statistically significant difference.
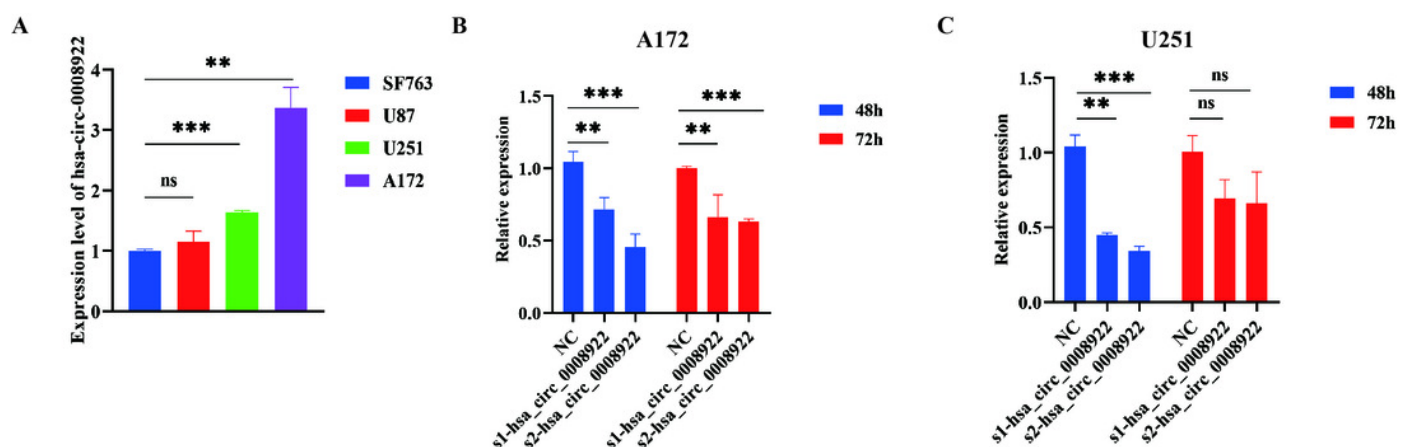
Figure 4

hsa_circ_0008922 regulates wound healing of A172 and U251 cells

(A and B) After down-regulation of hsa_circ_0008922 in A172, the scratch images at different time points were taken. (C and D) The quantitative results of scratch experiments in the NC group and the s2-has_circ_0008922 group in the A172 and U251 were counted. The ordinate is healing rate. The abscissa is the detection time point. s2-has_circ_0008922 represents the second siRNA fragments. Data is expressed as mean ± SEM. $**P < 0.01$, $***P < 0.001$.
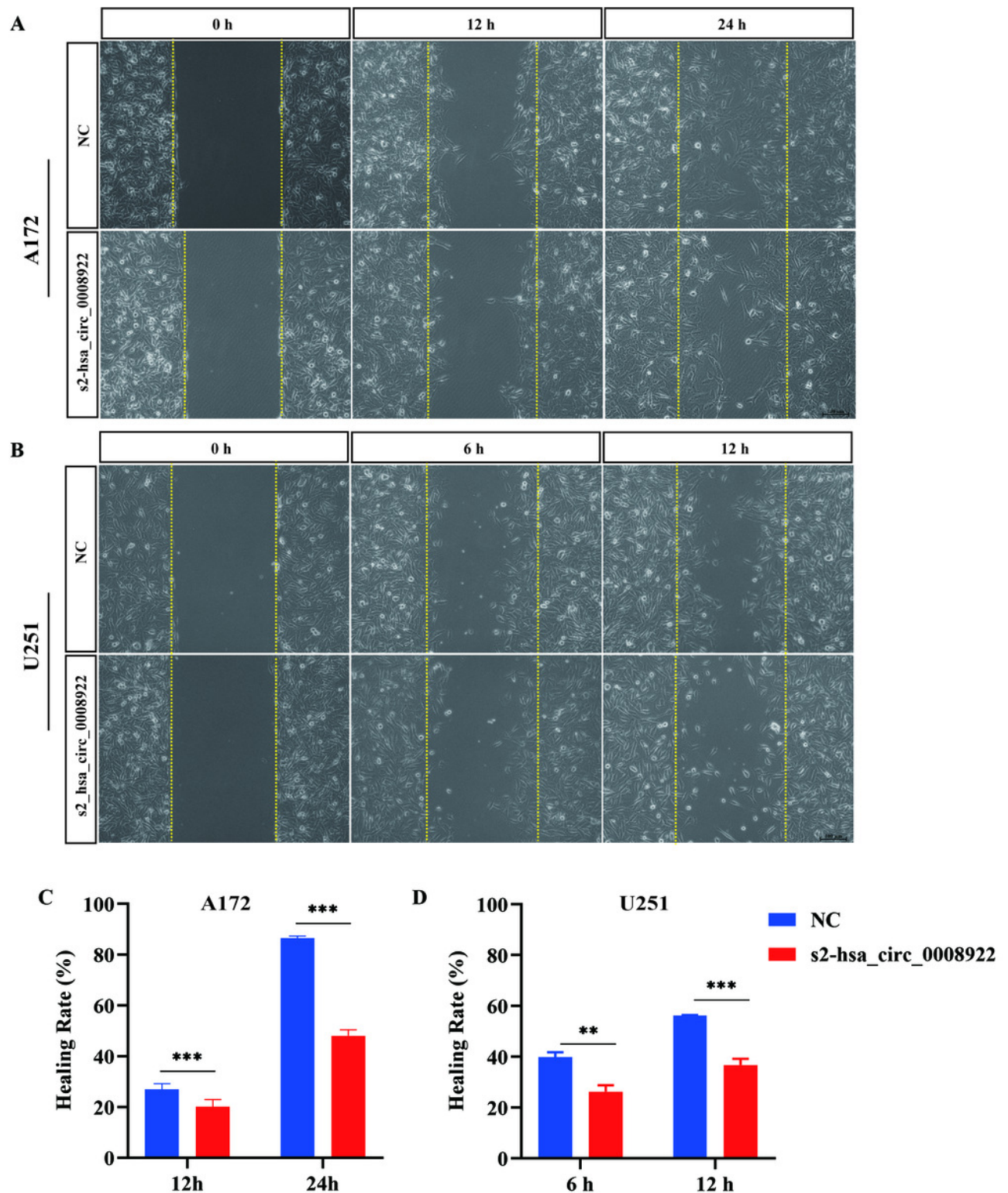
Figure 5

hsa_circ_0008922 attenuated migration and invasion of A172 and U251 cells

(A and D) After down-regulation of hsa_circ_0008922 in A172 and U251, the graphs of migration and invasion were taken. (B, C, D and F) After down-regulating hsa_circ_0008922 in A172 and U251, the quantitative results of migration and invasion experiments in NC group and s2-hsa_circ_0008922 group were counted. The vertical axis is the number of cells. s2-has_circ_0008922 represents the second siRNA fragments. Data is expressed as mean ± SEM. *P < 0.05, **P < 0.01.
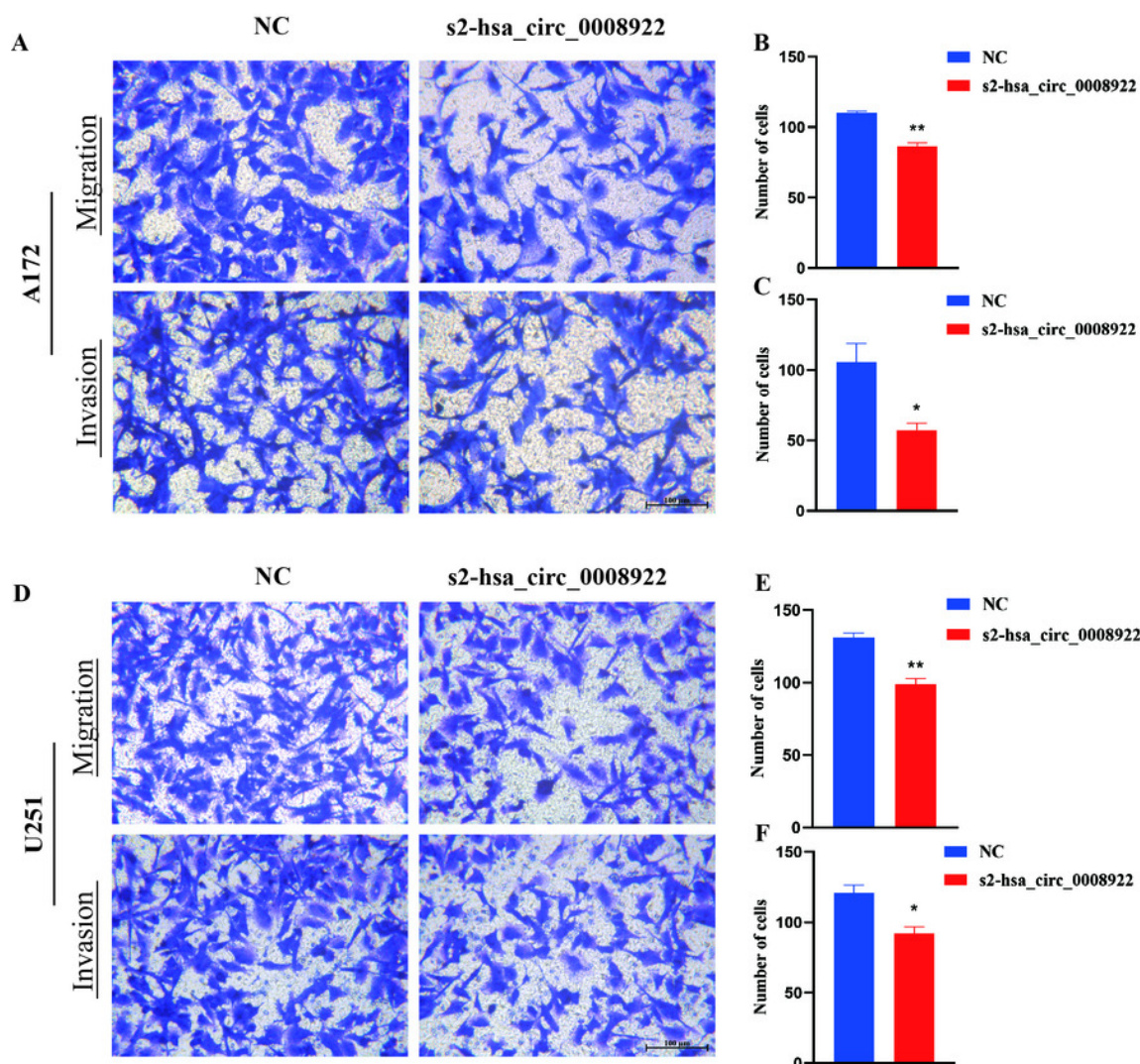
Figure 6

Down-regulation of hsa_circ_0008922 inhibited the colony formation and cell viability of A172 and U251 cells.

(A and B) Cell colony formation was detected by plate cloning after has_circ_0008922 was down-regulated in A172 and U251. (C and D) After down-regulating has_circ_0008922 in A172 and U251, cell viability was detected by CCK8. The ordinate is OD value. The abscissa is the detection time point (0 h, 24 h, 48 h, 72 h, 96 h). s2-has_circ_0008922 represents the second siRNA fragments. Data is expressed as mean ± SEM. *P < 0.05, **P < 0.01.
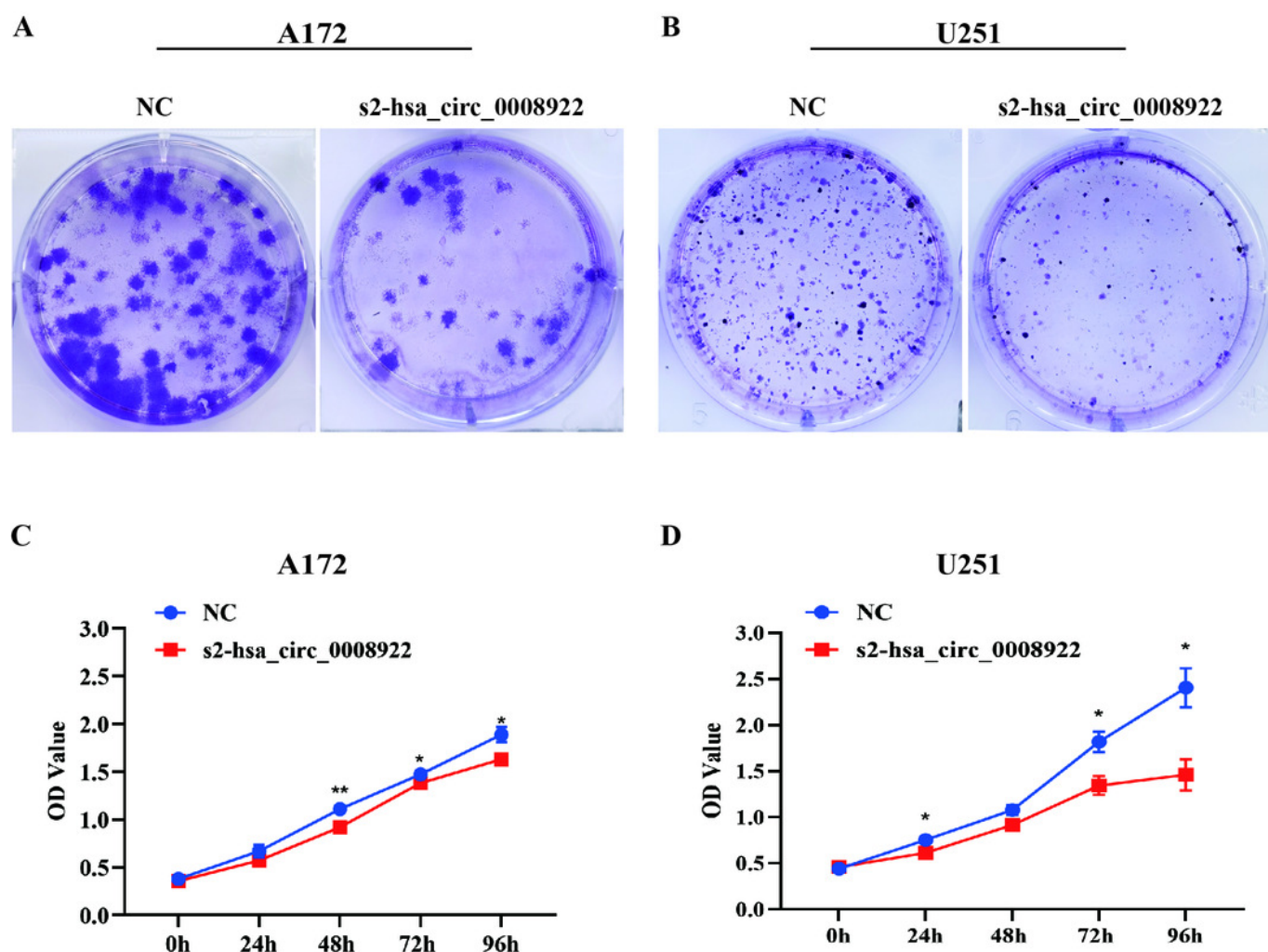
Figure 7

Down-regulation of hsa_circ_0008922 inhibited apoptosis of A172 and U251

.(A) Cell apoptosis was detected by flow cytometry after down-regulation of has_circ_0008922 in A172 and U251. (B and C) The apoptosis results of A172 and U251 were calculated. The ordinate is the apoptosis rate. (D) After down-regulating has_circ_0008922 in A172 and U251, WB was used to detect apoptosis-related protein expression. (E and F) The quantification results of A172 and U251 apoptosis protein were analyzed. The ordinate is the relative protein expression. The abscissa is the detected protein. s2-has_circ_0008922 represents the second siRNA fragments. Data is expressed as mean ± SEM. **$P < 0.01$, ***$P < 0.001$.
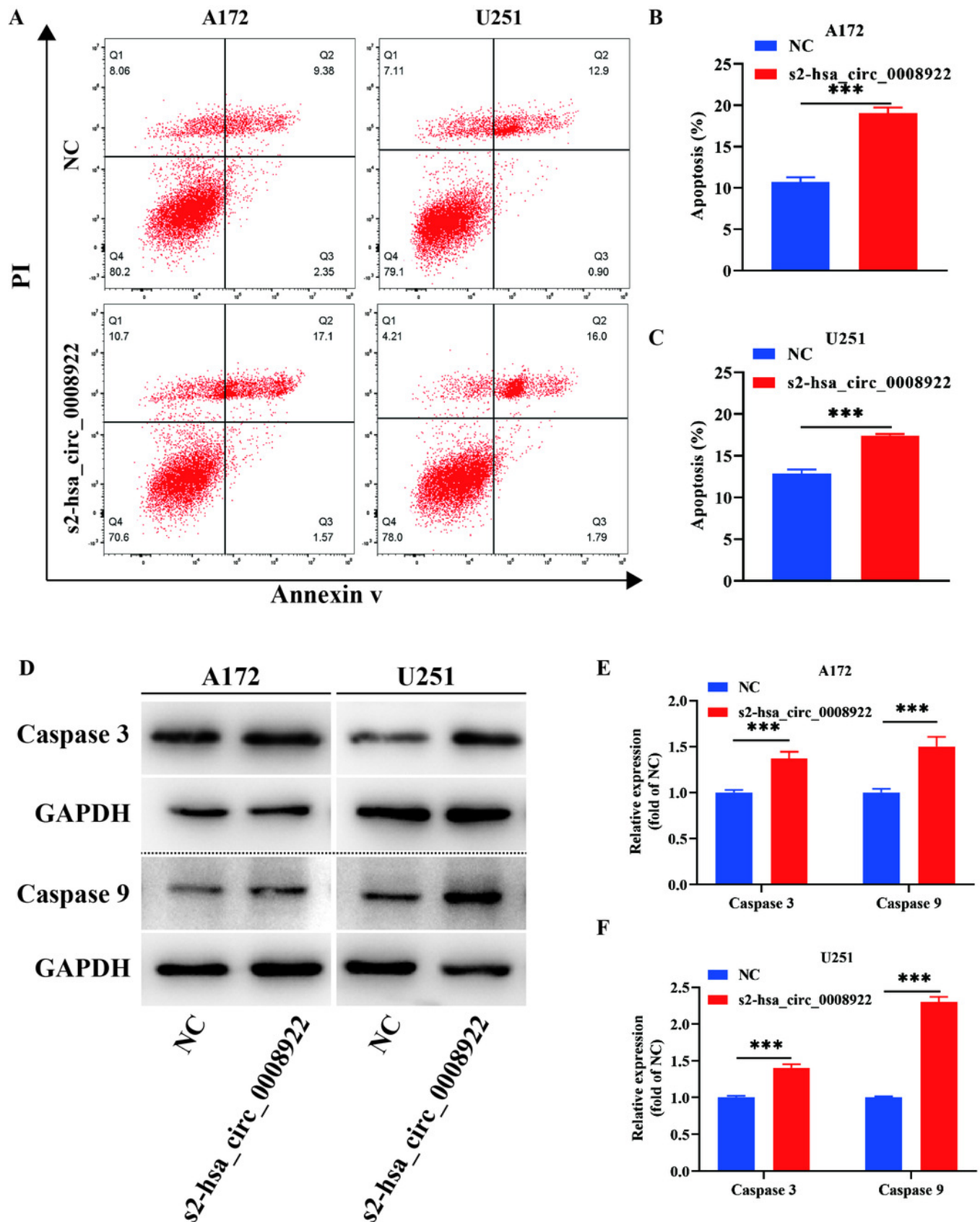
Figure 8

Prediction of the networks of circRNA-miRNA-mRNA

A) The interaction network between hsa_circ_0008922 and its downstream miRNAs was constructed. The blue square represents hsa_circ_0008922. Red circles indicate miRNAs. The line segment between the blue square and the red circle indicates a targeting relationship. The darker the line segment, the lower the predicted free energy, and the wider the line segment, the higher the predicted binding score. (B) Veen plots of mRNAs interacting with miRNAs downstream of hsa_circ_0008922 were drawn. Numbers in red circles indicate the number of mRNAs interacting with miRNAs in Linkedomics. Numbers in blue circles indicate the number of mRNAs interacting with miRNAs in miRDB. Numbers in green circles indicate the number of mRNAs interacting with miRNAs in miRWalk. (C) The interaction network between miRNA and its interacting mRNA was constructed. Red represents miRNA. white and blue represent mRNA; The larger the red circle, the higher the number of mRNAs interacting with the miRNA. The darker the circle, the higher the number of miRNAs interacting with the mRNA. The red line segment represents a positive correlation, and the wider the line segment, the stronger the positive correlation. The blue line segment represents a negative correlation, and the wider the line segment, the stronger the negative correlation.
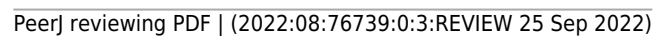
Figure 9

Analysis of the function of mRNAs negatively correlated with miRNAs

(A) A bubble plot of the top 30 enriched GO terms in mRNAs negatively correlated with miRNAs downstream of hsa_circ_0008922 was drawn. The y-axis represents the enrichment of the top 30 items, and the x-axis represents the enrichment score. The size of the bubbles indicates the number of mRNAs in the GO term. Bubble colors represent p-values. (B) A bubble plot of the top 30 enriched pathways in mRNAs negatively correlated with miRNAs downstream of hsa_circ_0008922 was drawn. The y-axis represents the enrichment of the top 30 items, and the x-axis represents the enrichment score. The size of the bubbles indicates the number of mRNAs in the pathway. Bubble colors represent p-values.
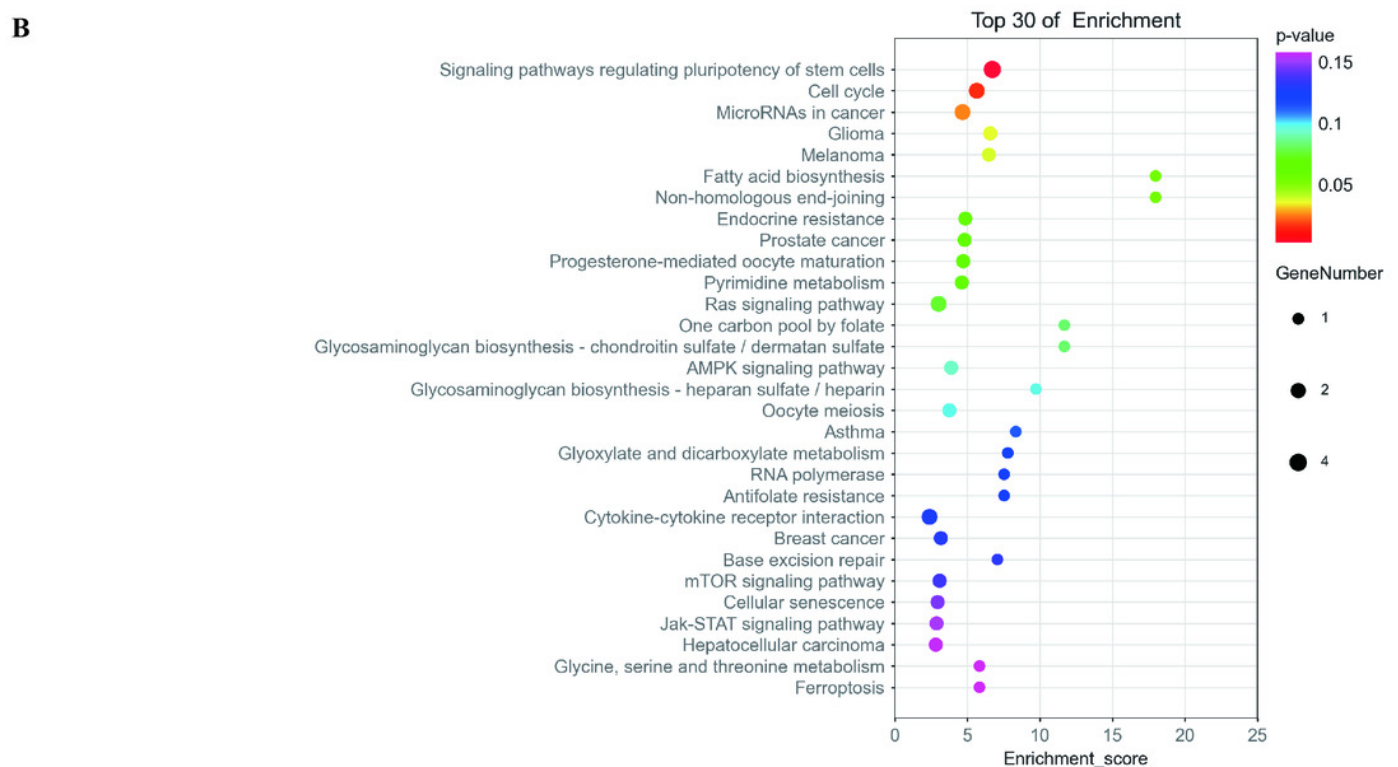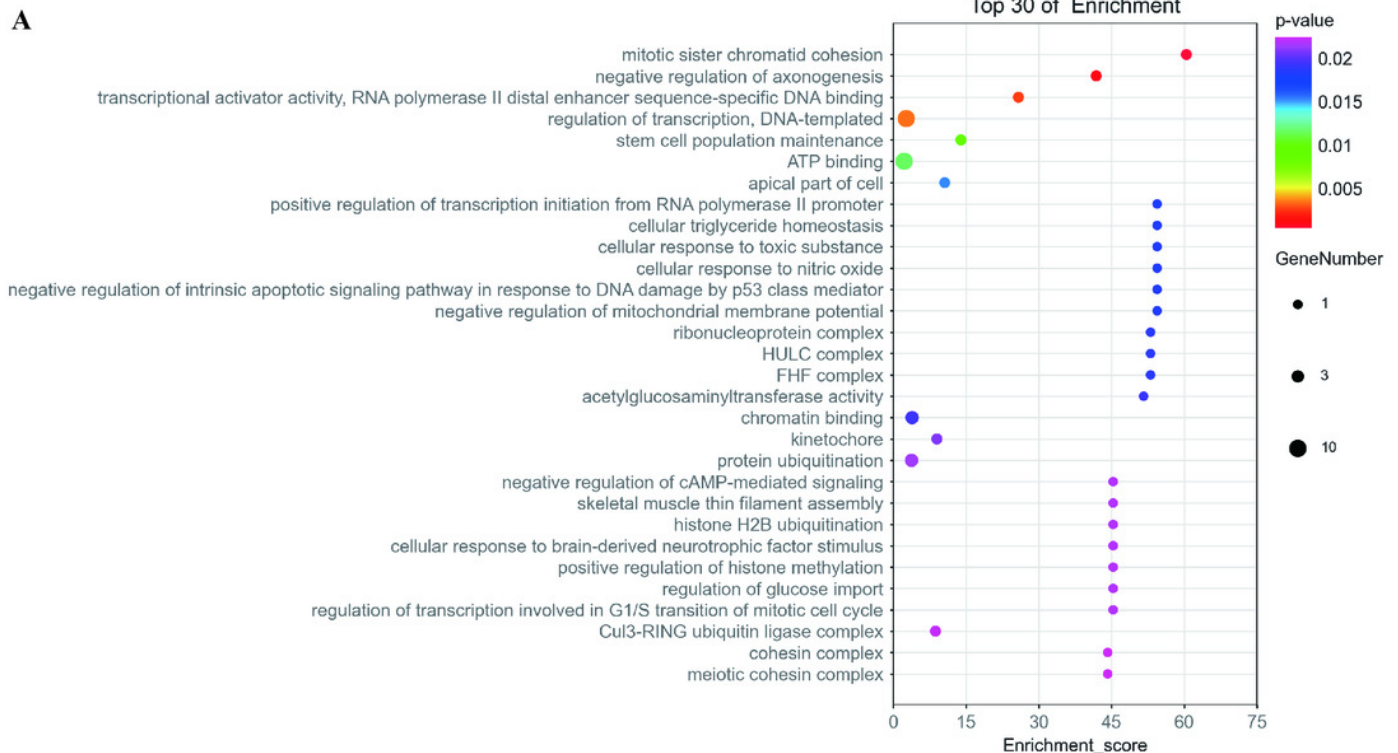
Table 1(on next page)

Clinicopathologic characteristics of GBM patients

GFAP: glial fibrillary acidic protein; P53: tumor protein p53; Ki67: marker of proliferation Ki-67; MGMT: O6-methyl-guanine DNA methyltransferase; KPS: Karnofsky Performance Status. IDH and 1p/19q COdeletion did not cover all specimens due to missing specimen information.

1 Table 1 Clinicopathologic characteristics of GBM patients

Items	Groups	Overall Information, n
Age (years)	< 42	20
	≥ 42	20
Gender	Male	23
	Female	17
Tumor size (diameter)	< 5 cm	20
	> 5 cm	20
WHO grade	Low grade（I-II）	21
	High grade（III-IV）	19
GFAP	- / +	40
	++ / +++	0
P53	- / +	28
	++ / +++	12
Ki-67	< 20 %	22
	≥ 20 %	18
MGMT	-	16
	+	24
KPS	< 70	14
	≥ 70	26
1p/19q codeletion	codeletion	6
	non-codeletion	1
IDH	Wt	12
	Mut	10

2 GFAP: glial fibrillary acidic protein; P53: tumor protein p53; Ki67: marker of proliferation Ki-67; MGMT: O6-

3 methyl-guanine DNA methyltransferase; KPS: Karnofsky Performance Status. IDH and 1p/19q COdeletion did

4 not cover all specimens due to missing specimen information.

5

Table 2(on next page)

Correlation between hsa_circ_0008922 expression and clinicopathological parameters of glioma patients

GFAP: glial fibrillary acidic protein; P53: tumor protein p53; Ki67: marker of proliferation Ki-67; MGMT: O6-methyl-guanine DNA methyltransferase; KPS: Karnofsky Performance Status. The relative expression of hsa_circ_0008922 was less than 3.8074, which was low expression. And conversely, it was high expression. ### indicated that statistical analysis cannot be carried out due to data distribution.

1   Table 2 Correlation between hsa_circ_0008922 expression and clinicopathological parameters of glioma patients

Items		hsa_circ_0008922 expression, n (%)		P
		Low	High	
Total		20	20	
Gender	Male	14 (70)	9 (45)	0.110
	Female	6 (30)	11 (55)	
Age (years)	< 45	13 (65)	11 (55)	0.519
	≥ 45	7 (35)	9 (45)	
Tumor size (diameter)	< 5 cm	18 (90)	2 (10)	0.000
	> 5 cm	2 (10)	18 (90)	
WHO grade	I-II	14 (70)	7 (35)	0.027
	III-IV	6 (30)	13 (65)	
GFAP	- / +	20 (100)	20 (100)	###
	++ / +++	0 (0)	0 (0)	
P53	- / +	15 (75)	13 (65)	0.49
	++ / +++	5 (25)	7 (35)	
Ki-67 (%)	< 20 %	16 (80)	6 (30)	< 0.001
	≥ 20 %	4 (20)	14 (70)	
MGMT	-	6 (30)	10 (50)	0.197
	+	14 (70)	10 (50)	
KPS	< 70	5 (25)	9 (45)	0.185
	≥ 70	15 (75)	11 (55)	

2   GFAP: glial fibrillary acidic protein; P53: tumor protein p53; Ki67: marker of proliferation Ki-67; MGMT: O6-

3   methyl-guanine DNA methyltransferase; KPS: Karnofsky Performance Status. The relative expression of

4   hsa_circ_0008922 was less than 3.8074, which was low expression. And conversely, it was high expression. ###

5   indicated that statistical analysis cannot be carried out due to data distribution.

6

Table 3(on next page)

Prediction of binding sites between miRNA and hsa_circ_0008922

Score: Score predicted by miranda; Energy: The free energy predicted by miranda; Target

Positions: The binding initiation site on hsa_circ_0008922.

1 Table 3 Prediction of binding sites between miRNA and hsa_circ_0008922

miRNA	Target	Score	Energy	miRNA Length	Target Positions
hsa-let-7e-5p	hsa_circ_0008922	158	-16.84	22	91
hsa-miR-506-5p	hsa_circ_0008922	155	-16.57	22	76
hsa-let-7b-5p	hsa_circ_0008922	154	-17.03	22	91
hsa-let-7c-5p	hsa_circ_0008922	154	-15.93	22	91
hsa-let-7g-5p	hsa_circ_0008922	154	-14.88	22	91
hsa-mir-98-5p	hsa_circ_0008922	150	-12	22	91
hsa-let-7d-5p	hsa_circ_0008922	150	-14.79	22	91
hsa-let-7i-5p	hsa_circ_0008922	147	-13.24	22	88
hsa-miR-377-3p	hsa_circ_0008922	143	-13.37	22	126
hsa-mir-605-3p	hsa_circ_0008922	157	-14.73	22	71
hsa-let-7a-5p	hsa_circ_0008922	158	-15.82	22	91
hsa-let-7f-5p	hsa_circ_0008922	150	-12	22	91
hsa-miR-4458	hsa_circ_0008922	156	-19.13	19	93
hsa-miR-4500	hsa_circ_0008922	146	-11.62	17	93

2 Score: Score predicted by miranda; Energy: The free energy predicted by miranda; Target Positions: The binding

3 initiation site on hsa_circ_0008922.

4